View metadata, citation and similar papers at core.ac.uk
brought to you by CORE
provided by Digital Library of the Czech Technical University in...

CZECH TECHNICAL UNIVERSITY IN PRAGUE

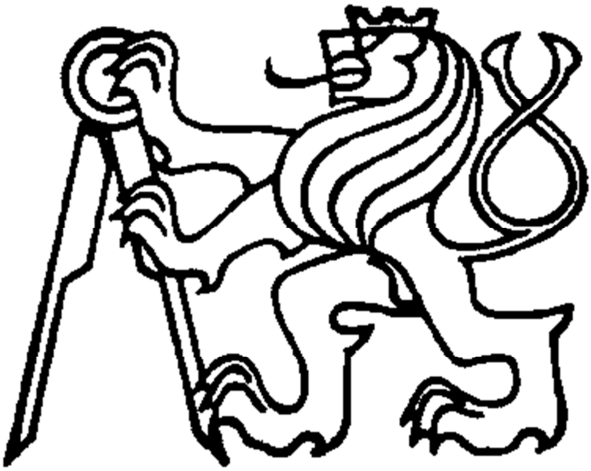

DOCTORAL THESIS STATEMENT

Czech Technical University in Prague

Faculty of Electrical Engineering

Department of Electromagnetic Field

Martin Válek

Radiation Model for Small Horizontal Submodules

Ph.D. Programme: Electrical Engineering and Information Technology

Branch of study: Radioelectronics

**Doctoral thesis statement for obtaining the academic title of "Doctor",
abbreviated to "Ph.D."**

Prague, July, 2011

The doctoral thesis was produced in combined manner Ph.D. study at the department of Electromagnetic Field of the Faculty of Electrical Engineering of the CTU in Prague.

Candidate:	Martin Válek
Establishment:	Dept. of Electromagnetic Field, Faculty of Electrical Engineering, CTU in Prague
Address	Technická 2, 166 27 Prague 6, Czech Republic
Supervisor:	Prof. Ing. Miloš Mazánek, CSc. Dept. of Electromagnetic Field Faculty of Electrical Engineering, CTU in Prague Technická 2, 166 27 Prague 6, Czech Republic
Supervisor-Specialist:	Prof. Dr.Ing. Marco Leone
Establishment:	Fakultät für Elektrotechnik und Informationstechnik Institute for Fundamental Electrical Engineering and EMC OTTO VON GUERICKE University of Magdeburg
Address:	Universitätsplatz 2, D-39106 Magdeburg, Germany

Opponents:

The doctoral thesis statement was distributed on:

The defence of the doctoral thesis will be held on at a.m./p.m. before the Board for the Defence of the Doctoral Thesis in the branch of study Radioelectronics in the meeting room No. of the Faculty of Electrical Engineering of the CTU in Prague.

Those interested may get acquainted with the doctoral thesis concerned at the Dean Office of the Faculty of Electrical Engineering of the CTU in Prague, at the Department for Science and Research, Technická 2, Praha 6.

Prof. Ing. Miloš Klíma
Chairman of the Board for the Defence of the Doctoral Thesis in the branch of study Radioelectronics
Faculty of Electrical Engineering of the CTU in Prague
Technická 2, 166 27 Prague 6, Czech Republic

1 INTRODUCTION

The State-of-Art methods keen to modular approach to electromagnetic compatibility (EMC) compliance evaluation in which the entire systems is split into separate modules and the EMC compliance is evaluated on the level of modules [15], [24]. However, the final qualification measurements and tests are still required to be performed on the entire system. Radio disturbance characteristics – Limits and methods of measurement – fall under the scope of International Special Committee on Radio Interference (CISPR) which is a subject matter group of International Electrotechnical Commission (IEC) [14]. Conclusions made below refer mainly to CISPR 22 recommendations [2], [3], [10]-[13].

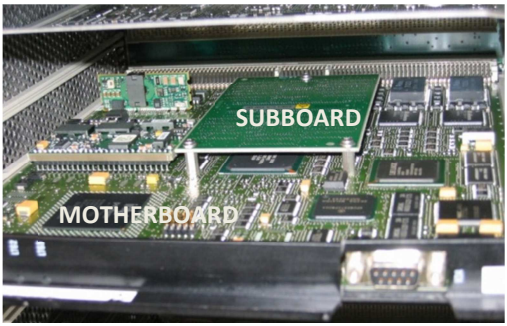

Fig. 1. Submodule-on-motherboard structure with grounding posts.

The subject to the investigations is a small horizontal submodule-on-motherboard (SB/MB) structure, see Fig. 1. A pre-assessment method which would allow to predict potential EMC issues on vertical SB/MB structures has been published in [21], [25] and [38], however, the field simulation is still needed for the determination of the antenna transfer function [17] ,[19], [20]. This doctoral thesis comes with a novel Radiation Model which allows to predict the magnitude of radiated electric field at the resonance of a small horizontal submodule and does not require any field simulation for the antenna transfer function. In order to further leverage from the fast prediction method, the computation exercise with Radiation Model can be combined with a measurement method in a shielded box.

2 GOALS & OBJECTIVES

Apart from a majority of design advantages, the submodules introduce serious challenges into the system, seen from EMC perspective. A submodule is an efficient radiator of the electric field.

The intention of this thesis is to

(i) describe the horizontal SB/MB structure in its entire complexity with a simple-to-solve Lumped-Element Equivalent Circuit;

(ii) derive a Radiation Model which allows to compute the electric field strength radiated from the structure by simply means of a circuit-analysis tool (e.g. PSPICE [32]) without a necessity of time consuming field simulations;

(iii) define some general rules to the design of interboard connector that leads to minimal risk of EMC non-compliance through an effective suppression of radiated electromagnetic interferences (EMI).

In addition, a novel method of practical evaluations of the radiated electric field in a shielded box is introduced that, together with the Radiation Model, demonstrates strong engineering potentials of the combined approach when comes to a pre-compliance assessment with respect to CISPR 22 requirements.

The principal goal is to provide with a method which allows the identification of potential design weaknesses of a small horizontal submodule already in the early design phase when no practical EMC measurements are possible.

3 RADIATION OF HORIZONTAL SUBMODULES

Although the SM/MB structure is a very popular design concept, it has been observed that it behaves as an unintentional radiator of electromagnetic fields [26] ,[24], [40]. Due to the non-negligible impedance of the signal-return path in the interboard connector, a small potential difference arises between the boards [8], driving the submodule reference plane against the motherboard ground as a very short monopole antenna. A magnitude of radiated fields may reach relatively high levels when harmonics of a high-

speed signal routed through the connector are close to the structure resonance frequency [40], [24], [28]. This feature can lead to significant issues with respect to the compliance to regulatory limits on EMI. A redesign of the electric equipment due to the non-conformance to EMC standards is very costly especially because of product design freeze during the qualification process prior the start of serial production. That is where the major motivation for engineers to deal with EMC issues originates from already in the early design phase of the electric equipment.

4 FIELD SIMULATION

The author comes with a novel method of estimation of the maximum electric field emitted by a horizontal submodule which is based on the numerical field simulation through the Method-of-Moments technique (MoM) [9], [29] while using a simplified model of the SB/MB structure. The numerical field simulations were performed with a full-wave field solver CONCEPT II [6].

4.1 Simulation Model

Submodules and motherboards are usually populated with numerous integrated circuits (ICs) and other components. As a good approximation, the motherboard and the subboard PCBs can be simply replaced by conductive surfaces [23].

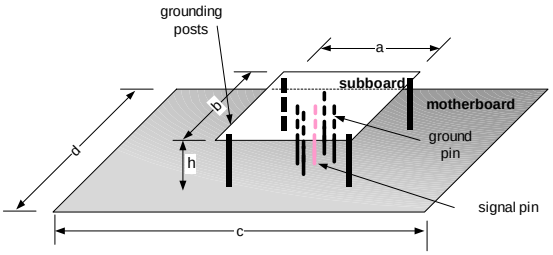

Fig. 2. Simplified model of SB/MB structure with grounding posts [34].

The schematic diagram in Fig. 2 simplifies the layout in order to indicate those entities and parameters used in mathematical expressions later in following chapters.

Let us consider PCB dimensions as given in Tab. 1 below. The connector pins are represented by round wires of the height h with the radius ρ. The connector pitch is s. Similarly, grounding posts are replaced by round conductors with the radius ρ' and height h.

Tab. 1. Geometrical parameters of the SB/MB structure for the computational examples.

DIMENSIONS	SUBMODULE-ON-MOTHERBOARD STRUCTURE
Motherboard	c = 23 cm, d = 22 cm
Subboard	a= 5 cm, b = 7 cm
Connector	h = 15 mm, s = 2.5mm, ρ = 0.4 mm
Grounding posts	h = 15 mm, ρ' = 1.5 mm

The representation of the interboard connector with uniform pin distance s corresponds to the typical connector configurations as shown in Fig. 3. The signal source is modelled by the Thévenin equivalent with source voltage V_s and internal impedance R_i.

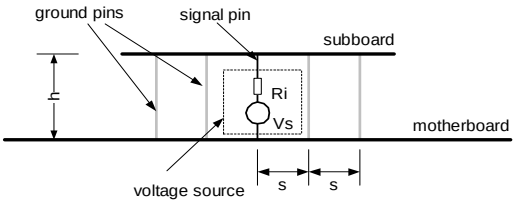

Fig. 3. Thévenin equivalent of the interboard connector.

To provide results of sufficient accuracy, the MoM requires a suitable discretization of the structure surface under consideration. This process is often called "*meshing*". The final meshing of the conductive surfaces which correspond to submodule and motherboard PCBs with parameters as per Tab. 1 is shown in Fig. 4. The accuracy of the simulations results can be extended through more advanced meshing of the structure surface with higher density of celling in the areas where the most current flow is expected.

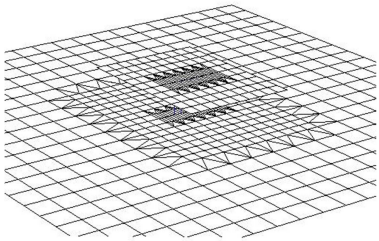

Fig. 4. Method-of-Moments (MoM). Meshing of the SB/MB structure.

In order to reduce the computation time, the number of unknowns can be minimized by replacing the finite motherboard ground plate (GP) with an infinite GP, based on Image Theory [1]. The computational example in Fig. 5 demonstrates the consequence of finite and infinite ground plane on the full-wave field simulation. The 6 dB correction factor represents the worst-case over-estimation while the simulations are carried out with an infinite reference plane.

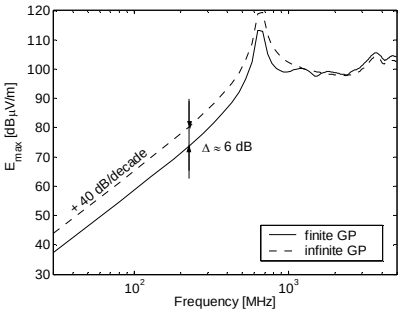

Fig. 5. Maximum radiated electric field at the distance of 3 meters from the structure. Interboard connector with only one signal and no ground pins (Vs = 1 Volt, Ri = 0Ω).

Below the first resonance, the radiation pattern is very similar to the one of a Hertzian dipole [27], [5], see Fig. 6a. The signal pin is located in the geometrical centre of the subboard.

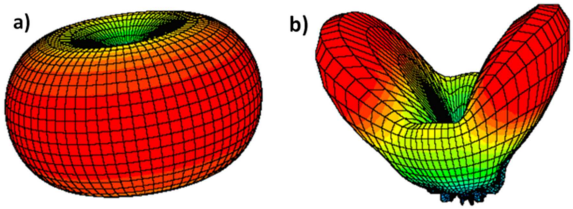

Fig. 6. E-field radiation pattern of the SB/MB structure in the far-field zone: a) in the low-frequency region (+40dB/decade), b) at the first cavity resonance $TM_{2,0}$.

The second resonance in Fig. 5 occurs at approximately 3.7 GHz. The second resonance is identified as a cavity-mode resonance of the subboard with radiation pattern as per Fig. 6b. Due to the central position of the signal pin, the first possible cavity resonance mode is the $TM_{2,0}$ mode which refers to the cavity resonator model in [16].

The frequency response of E_{max} changes when a return-current conductor (ground pin) is introduced in the interboard connector layout. By at least one ground pin in the connector, the E_{max} decays with 60 dB/decade towards lower frequencies as shown in Fig. 7.

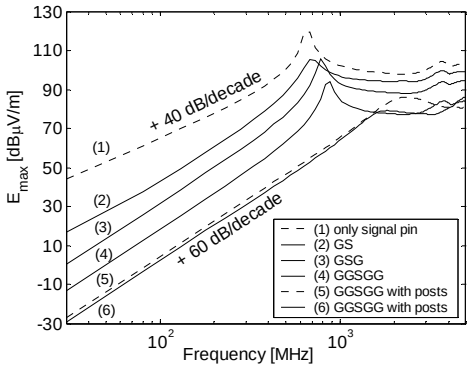

Fig. 7. Maximum radiated field for various connector and grouning posts layouts at the distance R of 3 meters. V_s = 1 Volt, R_i = 0 Ω (signal pin only), R_i = 50 Ω (signal and ground pins).

The maximum magnitude of the electric field E_{max} has been computed for several connector pin alignments using full-wave field solver CONCEPT II. Frequency responses of E_{max} are summarized in Fig. 7. The simulations have been performed for the structure dimensions as per Tab. 1 and the parameter values of connector Thévenin equivalent as follows: V_s = 1 Volt, R_i = 0 Ω (for the case of signal pin only), R_i = 50 Ω (for the case of signal and ground pins). The magnitude of E_{max} considerably decreases with increasing number of the ground pins. Most effective by the radiated emission suppression are the neighbour ground pins to the signal pin. The distance between the pins is critical, too. This is demonstrated in Fig. 8 for various pin distances *s*. This doctoral thesis shows that the more ground pins are available and the closer the ground pins are positioned mutually and towards the signal pin the tighter the current loops are and, hereby, the lower strengths of radiated electric field occur.

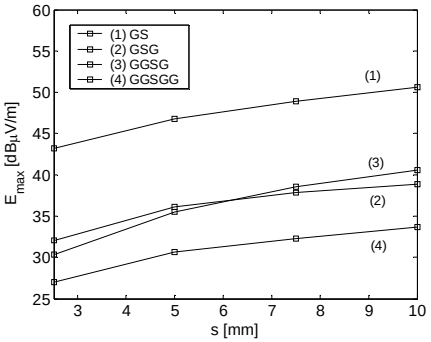

Fig. 8. Magnitude of E_{max} for various distances s between two neighbour pins in the free space and the observation distance R of 3 meters at the frequency of 100 MHz

5 RADIATION MODEL

In contrast to the numerical field simulations with an improved model, the Radiation Model is a novel approach to the radiated field estimation which is based on an analytical solution of Lumped-Element Equivalent Circuit of the interboard connector from [33], [22], and [32] extended with an Antenna Model. The Lumped-Element Equivalent Circuit and the Antenna

Model represent integral parts of the Radiation Model. The driving antenna voltage V_{ant} can be computed through a fast frequency analysis of the equivalent circuit and used for the field computations through the antenna representation. The main advantage of this approach is that only the commonly used circuit-analysis tools such as PSPICE [28] are needed to evaluate the EMI instead of more time consuming modelling concept with sophisticated field simulators.

The lumped-element circuit contains following parts:

- equivalent circuit of the interboard connector and,
- antenna model of a small horizontal submodule.

The physical characteristics of each part are described by means of lumped elements. The connector equivalent circuit is indicated in Fig. 9 and comprises self and mutual inductance of N pins L_{pN} and $M_{N,}$ resp., a signal source V_s and a total signal impedance Z_t while the antenna structure in Fig. 9 is represented by the electrical parameters R_{rad} and C_{ant}.

In order to assign the correct lumped element to each of the physical characteristics of the SB/MB structure further approximations are necessary.

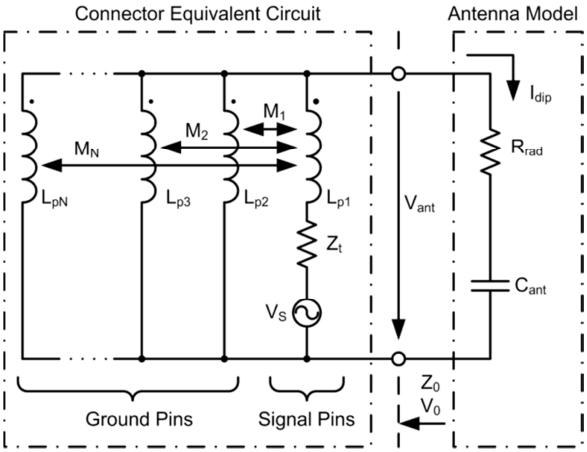

Fig. 9. The Lumped-Element Equivalent Circuit of small horizontal submodules [36]. Radiation Model.

The motherboard and the subboard are considered as perfectly conducting planes [23]. The connector pins may be simply represented by short wires [21], [35]. The wire length h corresponds to the height of the interboard connector. According to the concept of partial inductances [27], a segment of a conductor embodies an external inductance which can be expressed by means of a self-partial inductance. The self-partial inductance L_p of a pin with circular cross section can be computed from [27]

$$L_p = \frac{\mu_0}{2\pi} h \left[\ln\left(\frac{2h}{\rho} + \sqrt{\left(\frac{2h}{\rho}\right)^2 + 1} \right) + \frac{\rho}{2h} - \sqrt{\left(\frac{\rho}{2h}\right)^2 + 1} \right], \tag{1}$$

by known physical dimensions: the pin radius ρ and the connector height h. Each pin is coupled with all neighbouring pins by a mutual partial inductance M_n [21], [27]

$$M_n = \frac{\mu_0}{2\pi} h \left[\ln\left(\frac{2h}{n \cdot s} + \sqrt{\left(\frac{2h}{n \cdot s}\right)^2 + 1} \right) + \frac{n \cdot s}{2h} - \sqrt{\left(\frac{n \cdot s}{2h}\right)^2 + 1} \right], \tag{2}$$

where $n = 1, 2, 3 \ldots N$ is an integer index and s is the uniform pin separation as given by the connector pitch.

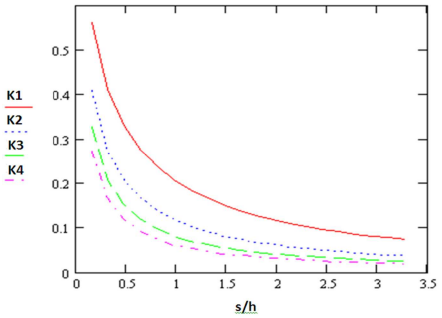

Fig. 10. Coupling factor K over the ration s/h.

The mutual coupling can be alternatively expressed by the coupling factor

$$K_n = \frac{M_n}{L_p}. \tag{3}$$

The mutual coupling M_n between two identical pins decreases exponentially with increasing multiple distance $n \cdot s$ between the pins as shown in Fig. 10.

With the reference to the $h/2$ rule [16] and in order to account for the fringing fields and by application of the image principle, the parameter C_{ant} can be expressed by the formula

$$C_{ant} \approx \varepsilon_0 \frac{(a+2h)(b+2h)}{h}, \tag{4}$$

where a and b are the dimensions of the subboard. The structure radiation resistance R_{rad} is given by one half of the radiation resistance of a Hertzian dipole [27], according to the image principle [22],

$$R_{rad} = 40\left(\frac{h}{c_0}\omega\right)^2. \tag{5}$$

For a worst-case estimation, only the maximum electric field strength E_{max} in the far field is considered. Accounting for the ground plane on the motherboard by the factor of two (image principle), E_{max} of a Hertzian dipole [27] is

$$E_{max} = 2 \cdot \frac{\mu_0 \omega h}{4\pi R} \cdot I_{dip}, \tag{6}$$

with the free space permeability μ_0 and the observation distance R. Expressing the dipole current I_{dip} by the antenna voltage V_{ant} and the capacitance C_{ant}, i.e.

$$I_{dip} = \frac{\omega C_{ant} V_{ant}}{\sqrt{(\omega C_{ant} R_{ant})^2 + 1}} \approx \omega C_{ant} V_{ant}, \tag{7}$$

we alternatively obtain

$$E_{max} = \frac{\mu_0 \omega^2 C_{ant} h}{2\pi R} \cdot V_{ant}. \tag{8}$$

The idea to separate the driving antenna voltage V_{ant} of the interboard connector from the antenna structure was mentioned in [21] for the very first time. However, the field simulations are still needed for the antenna transfer function in [21]. This doctoral thesis comes with an idea to approximate the antenna transfer function by the electric far field of a

Hertzian dipole [27], [1], [5]. The magnitude of V_{ant} determines the radiated electric field level E_{max}, according to the expression (8). The resonance frequency defines the peak in the frequency response of E_{max}. The antenna voltage V_{ant} from the equivalent circuit of the SB/MB structure (Fig. 9) can be computed with a customary circuit-simulation tool such as PSPICE. However, the value of the parameter R_{rad} must be found first. This requires an estimation of the resonance frequency ω_{res}. The relationship between the driving antenna voltage V_{ant} and the signal source V_s is

$$\frac{V_{ant}}{V_s} = \frac{\mathrm{j}\omega\Delta L}{Z_t\left[1-\left(\frac{\omega}{\omega_1}\right)^2\right] + 2\mathrm{j}\omega\Delta L\left[1-\left(\frac{\omega}{\omega_2}\right)^2\right]}, \tag{9}$$

where ω_1 and ω_2 are described with following formulas

$$\omega_1 = \frac{1}{\sqrt{L_p C_{ant}}}, \tag{10}$$

$$\omega_2 = \frac{1}{\sqrt{\frac{L_p + M}{2} C_{ant}}}. \tag{11}$$

The expression (10) and (11) identify the two limiting values for the resonance frequency ω_{res} of the transfer function (9). The actual location of ω_{res} lies within the interval (ω_1; ω_2). The situation is demonstrated in Fig. 11 for the parameters L_p, M and C_{ant} computed from the expressions (1), (2) and (4) and geometrical parameters of Tab. 1. An usual value of $Z_t = 50\ \Omega$ has been considered for the total signal impedance Z_t. Resonance frequency ω_2 can also be expressed in terms of the coupling factor K as follows

$$\omega_2 = \sqrt{\frac{2}{1+K}} \cdot \frac{1}{\sqrt{L_p C_{ant}}}. \tag{12}$$

Hence, the width of the resonance interval Δ is given by the relation

$$\Delta = \frac{\omega_2}{\omega_1} = \sqrt{\frac{2}{1+K}}. \tag{13}$$

The interval width Δ is strictly given by the coupling factor K which has values within the open interval (0; 1). Thus, ω_1 is the lower and ω_2 is the

upper limit resonance frequency. For the parameter values in Tab. 1 the interval width $\Delta = 1.13$ and it is again indicated in Fig. 11.

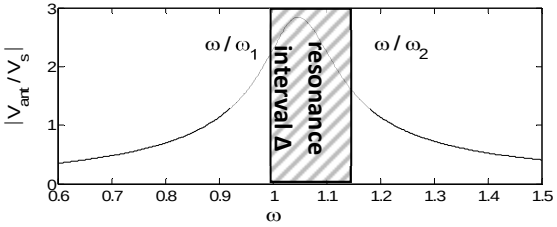

Fig. 11. The lower and the upper limits for the resonance frequency ω_{res} [32].

Should the resonance frequency ω_{res} occur close to the middle of Δ, the maximum uncertainty X with which the resonance frequency can be predicted is

$$X = \frac{\Delta - 1}{2} = \frac{(\omega_2 - \omega_1)/2}{\omega_1}. \tag{14}$$

5.1 Resonance frequency

The expressions (10) and (11) differ only by the inductance value, corresponding to the two limiting cases of the total pin inductance L_{tot}, depending on the value of Z_t:

$$\omega_1 = \frac{1}{\sqrt{L_{tot}^{N-1} C_{ant}}}, \tag{15}$$

$$\omega_2 = \frac{1}{\sqrt{L_{tot}^{N} C_{ant}}}, \tag{16}$$

where N is the number of all pins. Expressions (15) and (16) are applied for an arbitrary number of all connector pins with following approximations, in order to enable the derivation of a simple closed-form expression:

- All connector pins have the same self-partial inductance L_p (the same geometry)
- Only the contribution M_1 from the closest neighbour pin (by the outer pin) or pins (by the inner pin) is considered as shown in Fig. 12.

The actual occurrence of the resonance within the interval (ω_1; ω_2) is strongly given by the relationship between $|Z_t|$ and $\omega \cdot (L_p + M)$. However, the resonance frequency ω_{res} appears close to the middle of the interval (ω_1; ω_2) for the common values of Z_t, L_p and M. For the modelling approach introduced in this doctoral thesis, the arithmetic mean value of ω_1 and ω_2, as per expression (18), is an acceptable approximation for ω_{res}. Thereby, the resonance of the lumped-element model can be described with an approximate formula

$$\omega_{\text{res}} \approx \frac{1}{\sqrt{L_{tot} C_{ant}}}, \tag{17}$$

where

$$L_{\text{tot}} \approx \frac{1}{2}(L_{tot}^{N-1} + L_{tot}^{N}). \tag{18}$$

The total pin inductance L_{tot} in the case of the simplest connector configuration with one signal and only one ground pin $N_G = 1$ is

$$L_{\text{tot}} \approx L_p \frac{1}{2}\left(1 + \frac{1 + K_1}{2}\right). \tag{19}$$

The total pin inductance for the interboard connectors with more than one ground pin ($N_G > 1$) comes out as the complex solution of a system of equations and is different for each integer value of N_G.

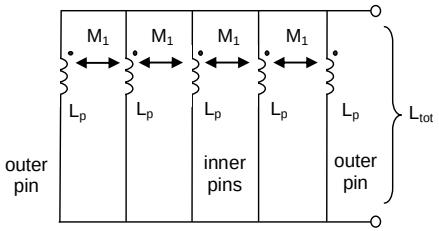

Fig. 12. Simplified coupling model of the connector, [33].

The author suggests an approximation with following formula [33]

$$L_{\text{tot}} \approx L_p \frac{1+K_1}{4}\left(\frac{1}{1+\frac{(N_G-2)(1+K_1)}{2(1+2K_1)}}+\frac{1}{1+\frac{(N_G-1)(1+K_1)}{2(1+2K_1)}}\right). \quad (20)$$

6 COMPUTATIONAL EXAMPLES

The simplest interboard connector configuration includes one signal and one ground pins.

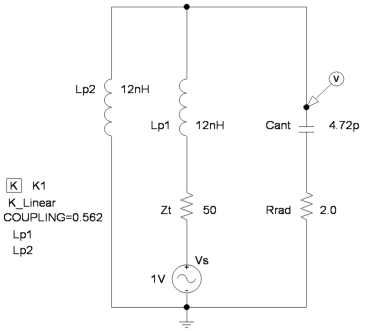

Fig. 13. PSPICE model of the SB/MB structure with a connector containing one signal and one ground pins.

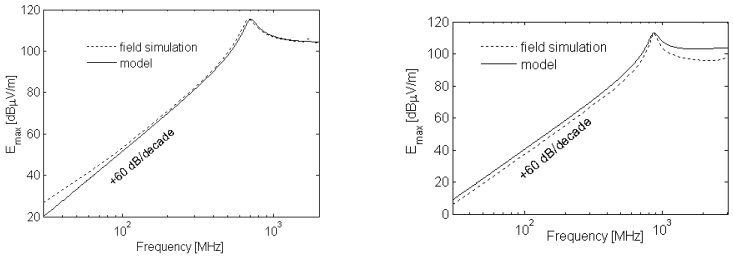

Fig. 14. Maximum electric field strength in the far field scaled to the 1 meter distance for a connector with a) one signal and one ground pins and b) one signal and four ground pins.

The corresponding PSPICE [28] circuit of the structure is shown in Fig. 13, with parameters calculated from the expressions (1) to (4), considering SB/MB parameters as per Tab. 1. Fig. 14 a) and b) show the resulting frequency response of E_{max}, scaled to the distance R of 1 meter from the structure. As a reference, the results of a full-wave field simulation through MoM were included. A very good correspondence of the presented model is observed.

7 EXPERIMANTAL EVALUATION

To the purpose of experimental validation a test board was designed which includes one submodule, see Fig. 15. The submodule is connected to the motherboard through an interboard connector of the same pitch as the one used for the computational examples in the previous section. All the design parameters of the test board are listed in Tab. 1.

a) b)

Fig. 15. Test-board for the experimental validation of the Radiation Model: a) construction with non-conductive posts [32]; b) The detailed view of the interboard connector [36].

7.1 Measurement setup

For purpose of the measurement presented in below sections the ground was covered with pyramidal absorbers so that only direct wave contributed to the electric field magnitudes measured on the receiver antenna. From these reasons, the measurement has been considered as being performed in the Free Space (FS) environment similar to anechoic chamber. The translation of measurement results into the Open Area Test Site emission levels (OATS) is done by accounting for a FS-to-OATS correction factor of 5dB [4], [8], [18], [37]. The test setup is shown in Fig. 16. In the simulations and

well as for the practical measurement, the signal amplitude of the voltage generator V_s was set to 22.3 mV.

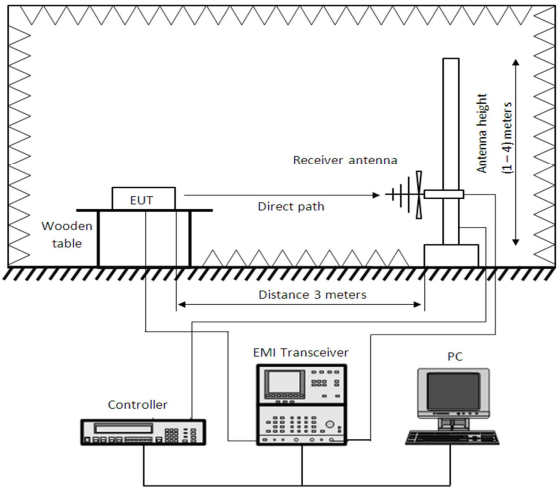

Fig. 16. Measurement setup.

7.2 Measurements results

Fig. 17 shows the comparison of the measurement results (solid line) with the results of the modelling approach (dotted line) and the field simulation (dash-dot line).

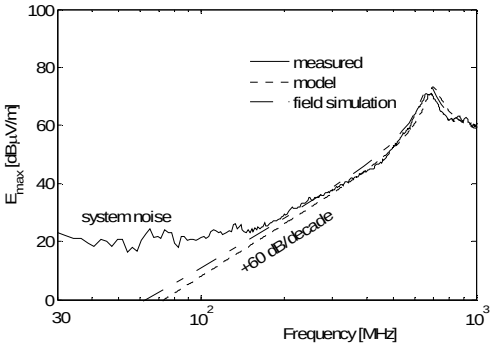

Fig. 17. Experimental validation of the suggested modelling approach [33].

Below 300 MHz, the small radiation level is overlapped by the system noise. Considering an usual emission measurement uncertainty of around

1.5 dB as well as parameter tolerances of the test board, an acceptable overall correspondence is obtained.

8 COMBINED METHODS

A shielded box is used for a measurement of radiated emissions from a small submodule. The space within the box is limited, especially, while absorbers are used to minimize the reflections from the metallic walls.

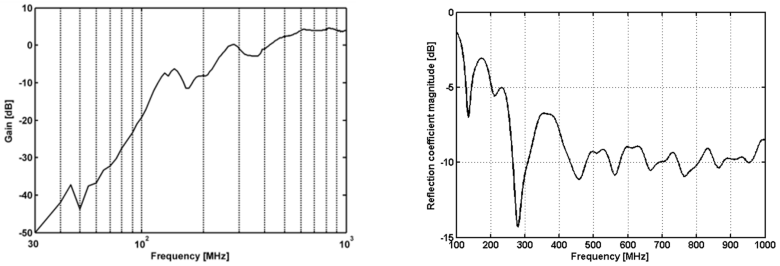

a) b)

Fig. 18. Planar spiral antenna: a) Gain G_r as measured in the shielded box [36]; b) Magnitude of the reflection coefficient S_{11}.

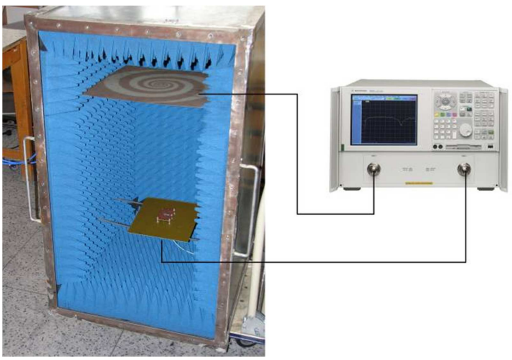

Fig. 19. Experimental validation in the shielded box [33].

Wideband planar spiral antenna [26], [30] was used for the EMI measurement in order to further leverage the advantages of measurement in a shielded box. The gain G_r as well as the magnitude of receiver antenna reflection coefficient S_{11} were measured in the box by the method of two

identical antennas. See Fig. 18 for the values of G_r and S_{11}. The measurement setup is in Fig. 19.

8.1 Measurement results

The measurement results for the electric field magnitude E_{max} [dBV/m], scaled to OATS levels in 3 meters distance is presented in Fig. 20 (dash-dotted line). The expression for E_{max} is as follows

$$E_{max}[\mathrm{dBV/m}] = V_{ant}[\mathrm{dBV}] + AF_r[\mathrm{dB/m}] - L_{total}[\mathrm{dB}], \tag{21}$$

where L_{total} includes various losses as follows

$$L_{total}[\mathrm{dB}] = L[\mathrm{dB}] + L_{pol}[\mathrm{dB}] - L_{FS-to-OATS}[\mathrm{dB}]\,. \tag{22}$$

The computational results using the Radiation Model and the field measurements in the shielded box are compared with the measurements in the anechoic chamber translated to OATS values. The comparison scaled to 3 meters distance and signal source V_s of 22.3mV is shown in Fig. 20.

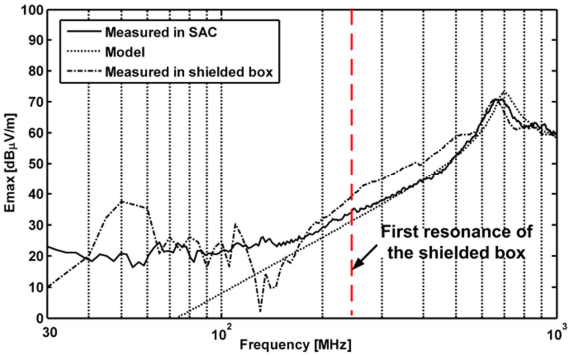

Fig. 20. Magnitude of radiated electric field in a distance of 3 meters [36].

Apparently, the planar spiral antenna does not perform sufficiently on the frequencies below 200 MHz. The first self resonance of the shielded box occurs at 261 MHz. There is roundly 6 dB add-on on the E_{max} in the frequency range of 250 - 580 MHz which is caused by low operation

effectiveness of the λ/4 pyramidal absorbers of the height of 12 centimetres (higher absorber effectiveness is expected first from frequency of 625 MHz).

The overall maximum field strength at 670 MHz has been identified by both the approaches the measurement in a shielded box and the radiation model. The combined approach is recommended in order to prevent against situations in which the critical EMC events appear outside the frequency range applicable for the planar spiral antenna.

9 CONCLUSIONS

9.1 Achievements

With respect to Goals & Objectives set upfront to this doctoral thesis, the author comes with novel suggestions and conclusions as follow:

(i) The subomule-on-motherboard structure can be described with Lumped-Element Circuit which includes the equivalents of the interboard connector and the Antenna Model of the SB/MB structure. The Antenna Model and the Lumped-Element Circuit build Radiation Model. The interboard connector has an inductive character which originates in the system of self-partial inductances of all pins while the antenna nature of the SB/MB structure is mainly capacitive due to the capacitance between the boards. The series of total pin inductance and the antenna capacitance gives a rise to a series resonance which is subject to EMI investigations.

(ii) The magnitude of the radiated electric field can be computed from the antenna voltage which comes out as a result of the Lumped-Element Equivalent Circuit analysis. There is no need of field simulation which is the main differentiator of the modelling approach through Radiation Model.

(iii) The design of the interboard connector is crucial in EMI suppression. Both the Radiation Model and the Field Simulations shows that the more ground pins are available and the closer they are to the signal pin in terms of connector pitch the less the electric field is effectively radiated by the

structure. Grounding posts will further prevent against cavity resonances.

(iv) The Radiation Model enables a prediction in the phase when no samples are available yet. However, once some samples are available, it may be worth to perform some practical measurements in order to check the EMI profile. This doctoral thesis introduces a method which is an unique combination on the modelling approach and practical measurements in a shielded box while planar spiral antenna is in use. The planar spiral antenna is wideband and fits into the box, however prior a check with Radiation Model is necessary in order not to miss the resonance of the SB/MB structure in the frequency range where the planar spiral antenna does not perform efficiently, typically on frequencies of tens of megahertz.

9.2 Potentials for Further Investigations

As it was confirmed by the field simulations, the EMI of submodules can be effectively suppressed by introduction of grounding posts into the design. Further development of the Lumped-Element Equivalent Circuit of the SB/MB structure shall include equivalents for grounding posts.

The expression (67) for the total pin inductance L_{tot} considers the mutual coupling K_n for level 1, i.e. $n = 1$, which practically means that only neighbour pins are accounted. In the next step, the analytical expression for L_{tot} shall be extended for the case of $n > 1$. The computation of L_{tot} may also be automated so that the results with higher accuracy are available immediately.

List of literature used in the thesis statement

[1] BALANIS, C.A. *Antenna Theory*. John Wiley & Sons, Inc., New York, 1997.

[2] CISPR 16-2: 2003. *Part 2 – Methods of measurement of disturbances and immunity.* Radiated Disturbance Measurement. 2003-07. CISPR 2003.

[3] CISPR 22: 2003-04. *Information technology equipment – Radio disturbance characteristics – Limits and methods of measurement*. 2003-04. CISPR 2003.

[4] CLAY, S. "Improving the Correlation between OATS, RF Anechoic Room and GTEM Radiated Emissions Measurements for Directional Radiators at Frequencies between approximately 150 MHz and 10 GHz". *IEEE 1998*, 0-7803-5015-4/98.

[5] PAUL, R. C.; WHITES, K. W.; NASAR, S. A. *Introduction to Electromagnetic Fields*. McGraw-Hill, 1998.

[6] CONCEPT II. 3D field simulator. CONCEPT II is accessible on the home page of Institute of Electromagnetic Theory at the Technische Univeristät Hamburg-Harburg; http://www.tet.tu-harburg.de/concept/index.en.html.

[7] FORNBERG, P.E.; KANDA, M.; LASEK, C.; PIKET-MAY, M.; HALL, S.H. "The impact of nonideal return path on differential signal integrity", *IEEE Trans. Electromagnetic Compatibility*, vol. 44, no. 1, Feb. 2002.

[8] GERMAN, R.F., "Comparison of semi-anechoic chamber and open-field site attenuation measurements". *IEEE International Symposium Record on Electromagnetic Compatibility*, 1982, pp 260-265.

[9] HARRINGTON, R. F. *Field Computation by Moment Methods.* New York, IEEE Press, 1993.

[10] IEC 61000-4-20: 2003. *Electromagnetic Compatibility (EMC) - Part 4-20: Testing and measurement techniques - Emission and immunity testing in transverse electromagnetic (TEM) waveguides*. IEC 2003.

[11] IEC 61967-1: 2002. *Part 1 – General conditions and definitions.* Integrated circuits – Measurement of electromagnetic emissions, 150 kHz to 1 GHz. 2002-03. IEC 2002.

[12] IEC 61967-2: 2003. *Part 2 – TEM-Cell Method*. Integrated circuits – Measurement of electromagnetic emissions, 150 kHz to 1 GHz. 2003-12. IEC 2003.

[13] IEC 61967-3: 2003. *Part 3 – Surface scan method.* Integrated circuits – Measurement of electromagnetic emissions, 150 kHz to 1 GHz. 2003-12. IEC 2003.

[14] International Electrotechnical Commission (IEC). IEC web site www.iec.ch.

[15] KODALI, V. P. *Engineering Electromagnetic Compatibility*. 2nd ed. IEEE Press, 2001.

[16] LANGE, K.; LÖCHERER, K.-H. *Taschenbuch der Hochfrequenztechnik*, Springer-Verlag, 1986.

[17] LEFERINK, F. B. J., "Reduction of printed circuit board radiated emission", *IEEE Int. Symp. Electromagnetic Compatibility*. 1997, pp. 431-438.

[18] LEFERINK, F.B.J; GROOT-BOERLE, D.J.; PUYLAERT, B.R.M. “OATS Emission Data Compared with Free-Space Emission Data”. *IEEE Intl. Symp. EMC. Atlanta*, GA, pp.333-337, 1995.

[19] LEONE, M. “Berechnung des Ein- und Abstrahlungsverhaltens von Leiterplatten mit der Momentenmethode“. *VDI Verlag*. Düsseldorf 2000.

[20] LEONE, M. “Ermittlung des Gleichtakt-Abstrahlungspegels von Leiterplatten unter Berücksichtigung von angeschlossenen Kabeln“. *Intl. Sym. EMV*. Düsseldorf, Germany. 2002.

[21] LEONE, M.; NAVRÁTIL, V. “On the electromagnetic radiation of printed-circuit-board interconnections”. *IEEE Transactions on Electromagnetic Compatibility*, May 2005, vol. 47, no. 2, pp.219 - 226.

[22] LEONE, M.; VALEK, M. “Netzwerkmodell für die Strahlungsanalyse von horizontalen Leiterplatten-Submodulen“. *EMV 2008, Internazionale Fachmesse und Kongress für elektromagnetische Verträglichkeit*. Düsseldorf. Germany. 2008. Awarded with BEST PAPER AWARD

[23] LI, K., TASSOUDIJ, A.; POH, S.Y; TSUK, M.; SHIN, R.T.; KONG, J. A. “FD-TD Analysis of Electromagnetic Radiation from Modules-on-Backplane Configurations”. *IEEE Transactions on Electromagnetic Compatibility*. Aug. 1995, vol. 37, no 3, pp.326 - 332.

[24] MONTROSE, M.I. *Printed Circuit Boards Design Techniques for EMC Compliance*. IEEE Press. New York. 1996.

[25] NAVRÁTIL, V. *Modelling of Magnetic-coupled Radiation Mechanism in Electronic Systems*. Doctoral Thesis. September 2004. Brno University of Technology. Brno. Czech Republic.

[26] PIKSA, P.; MAZANEK, M. “A self-complementary 1.2 to 40 GHz spiral antenna with impedance matching”. *Radioengineering*. Vol. 15, no. 3, pp. 15-19, Sept. 2006.

[27] PAUL, C. R. *Introduction to Electromagnetic Compatibility*. John Wiley & Sons, Inc., New York, 1992.

[28] PSPICE. Personal Simulation Program with Integrated Circuit Emphasis. Analog and mixed-signal circuit simulator. *Cadence*. Available on Cadence Home Page: http:// www.cadence.com.

[29] SINGER, H.; BRÜNS H.D.; BÜRGER G. “State of the Art in the Method of Moments”. *IEEE Int. Symp. Electromagnetic Compatibility and 4 Years Symposia Records 1999*. Seattle, USA, published 1996 pp.122-127.

[30] KORINEK, T.; PIKSA, P.; MAZANEK, M. “Wideband Measurement in a Small Shielded Box Using Equiangular Spiral Antennas”. *Radioengineering*, vol. 15, no. 4, pp. 34-37, Sept. 2006.

[31] RAPPAPORT, T. S.. *Wireless Communications - Principles and Practice*. 2nd. ed., Prantice Hall, 2002, p. 177 - p253.

[32] VÁLEK, M.; LEONE, M. “Estimation of Radiated Fields of Small Horizontal Submodules Based on a Lumped-Element Model”. *Radioengineering*. 2006. Vol. 15, no. 4, p. 9-15. ISSN 1210-2512.

[33] VÁLEK, M.; LEONE, M. “Radiation Model for Small Horizontal Submodules”. *In Proceedings of the VII EMC Europe.* Barcelona (Spain), 2006, p.426-430. ISBN: 84-689-9438-3

[34] VALEK, M.; LEONE, M.; SCHMIEDL, F. “Analysis of the radiation behaviour of motherboard-subboard structures”. *Proc. of the 6th International Symposium on Electromagnetic Compatibility and Electromagnetic Ecology*. June 21-24, 2005, St.-Petersburg, Russia, pp.175-178.

[35] VALEK, M.; LEONE, M.; SCHMIEDL, F. “Simulation of the Unintentional Radiated Interference of Electronic Modules”. *Radioelektronika 2005 - Conference Proceedings*. Brno, Czech Republic: FEEC BUT, Dept. of Radio Electronics, 2005, p. 243-246. ISBN 80-214-2904-6.

[36] VALEK, M.; KORINEK, T.; MAZANEK, M. “Pre-Assessment of Radiated Fields from Small Electronic Submodules”. Submitted to *IEEE Transactions on Electromagnetic Compatibility*. Manuscript registered under ID TEMC-142-2011 in June 2011.

[37] VALEK, M.; LEONE, M. “Radiated Emission Measurement of Printed Circuit Boards in he GTEM Cell andd GTEM-to-OATS Correlation Factor“. *Proceedings of COMITE 2005.* IEEE Czechoslovakia Section. Praha. 2005. ISBN 80-86582-16-7.

[38] YE, X.; NADOLNY, J.; DREWNIAK, J.L.; HOCKANSON, D.M. “High-performan-center-PCB connectors: Analysis of EMI characteristics“. *IEEE Trans.Electromagnetic Compatibility*, vol. 44, no. 1, Feb. 2002, pp. 165-174.

List of candidate's works related to the doctoral thesis

Journal Articles

[1] VÁLEK, M.; LEONE, M. "Estimation of Radiated Fields of Small Horizontal Submodules Based on a Lumped-Element Model". *Radioengineering.* 2006. Vol. 15, no. 4, p. 9-15. ISSN 1210-2512.

[2] VALEK, M.; KORINEK, T.; MAZANEK, M. "Pre-Assessment of Radiated Fields from Small Electronic Submodules". Submitted to *IEEE Transactions on Electromagnetic Compatibility.* Manuscript registered under ID TEMC-142-2011 in June 2011.

International Conference Papers

[1] LEONE, M.; VALEK, M. "Netzwerkmodell für die Strahlungsanalyse von horizontalen Leiterplatten-Submodulen". *EMV 2008, Internazionale Fachmesse und Kongress für elektromagnetische Verträglichkeit*. Düsseldorf. Germany. 2008. Awarded with BEST PAPER AWARD

[2] VÁLEK, M.; LEONE, M. "Radiation Model for Small Horizontal Submodules". *In Proceedings of the VII EMC Europe*. Barcelona (Spain), 2006, p.426-430. ISBN: 84-689-9438-3

[3] VALEK, M.; LEONE, M.; SCHMIEDL, F. "Analysis of the radiation behaviour of motherboard-subboard structures". *Proc. of the 6th International Symposium on Electromagnetic Compatibility and Electromagnetic Ecology.* June 21-24, 2005, St.-Petersburg, Russia, pp.175-178.

[4] VALEK, M.; LEONE, M.; SCHMIEDL, F. "Simulation of the Unintentional Radiated Interference of Electronic Modules". *Radioelektronika 2005 - Conference Proceedings.* Brno, Czech Republic: FEEC BUT, Dept. of Radio Electronics, 2005, p. 243-246. ISBN 80-214-2904-6.

[5] VALEK, M.; LEONE, M. "Radiated Emission Measurement of Printed Circuit Boards in the GTEM Cell andd GTEM-to-OATS Correlation Factor". *Proceedings of COMITE 2005.* IEEE Czechoslovakia Section. Praha. 2005. ISBN 80-86582-16-7.

[6] VALEK, M., KORINEK T, BOSTIK T." Design of stripline for EMC testing" *COMITE. 14th International Conference on Microwave Techniques.* Apr 23-24, 2008, Prague. Czech Rep. 2008, Pages: 203-206, Published: 2008.

Awarded paper

LEONE, M.; VALEK, M. "Netzwerkmodell für die Strahlungsanalyse von horizontalen Leiterplatten-Submodulen". *EMV 2008, Internazionale Fachmesse und Kongress für elektromagnetische Verträglichkeit.* Düsseldorf. Germany. 2008.

In case of shared authorship the co-authors contributed equally.

Response

Following paper

VALEK, M.; LEONE, M.; SCHMIEDL, F. “Analysis of the radiation behaviour of motherboard-subboard structures”. *Proc. of the 6th International Symposium on Electromagnetic Compatibility and Electromagnetic Ecology*. June 21-24, 2005, St.-Petersburg, Russia, pp.175-178.

was cited in

[1] FRIEDRICH, M.; LEONE, M.: “Network model for the analysis of radiated emissions from horizontal PCB submodules”. *IEEE International Symposium on Electromagnetic Compatibility*. Piscataway, NJ : IEEE, ISBN 978-1-424-46307-7, S. 631-636, 2010. Congress: IEEE EMC; (Fort Lauderdale, Florida) : 2010.07.25-30.

[2] KOBAYASHI, N; HARADA, T.. “An investigation of the effect of chassis connections on radiated EMI from PCBs”. *2006 IEEE International Symposium on Electromagnetic Compatibility*. Proceedings, vols 1-3, pp. 275. Published 2006. 1-4244-0293-X (c)2006 IEEE.

And the papers as follows

[1] VÁLEK, M; ZVÁNOVEC, S; - PECHAČ, P.. ”Indoor Propagation Measurement for Wireless Systems Operating in 2.45 GHz ISM Band”. *Radioengineering. 2002*, vol. 11, no. 4, p. 48-52. ISSN 1210-2512.

[2] ZVÁNOVEC, S; VÁLEK, M; PECHAČ, P. ”Results of Indoor Propagation Measurement Campaign for WLAN Systems Operating in 2.4 GHz ISM Band”. *In Antennas & Propagation - Twelfth International Conference. ICAP 2003*. London: IEE, 2003, p. 63-66. ISBN 0-85296-752-7.

were cited in

[1] SUJAK, B.; GHODGAONKAR D.K.; ALI, B.M. ”Indoor propagation channel models for WLAN 802.11b at 2.4GHz ISM band”. *In APACE: 2005 Asia-Pacific Conference on Applied Electromagnetics*, Proceedings, 2005.

[2] LEE S.: Park Y.; Yu J.. “Performance of WLAN 802.11b standard at in-vehicle environment”. *In 2006 6th International Conference on ITS Telecommunications.* Proceedings, 2006.

[3] MELIA T.; OLIVA, A.; Soto, I.. “Analysis of the effect of mobile terminal speed on WLAN/3G vertical handovers”. *In GLOBECOM 200. 2006 IEEE Global Telecommunications Conference, 2006*. ISSN 1930-529X.

[4] SASLOGLOU, K.; DARBARI, F.; GLOVER, I.A..”Some Preliminary Short-Range Transmission Loss Measurements For Wireless Sensors Deployed On Indoor Walls”. *In 2008 11th IEEE Singapore International Conference On Communication Systems (ICCS)*, vols 1-3, 2008.

[5] SMADI, M.; AZHARI, V.S.; TODD, T.D.; KEZYS, V.. “A Study of WLAN-to-Cellular Handover Using Measured Building-Exit Data.” *In IEEE Transactions on Vehicular Technology*, 2009. ISSN 0018-9545.

[6] ANDRADE, C.B.; HOEFEL, R.P.F..”IEEE 802.11 WLANS: A Comparison on Indoor Coverage Models.” *In 2010 23RD Canadian Conference on Electrical and Computer Engineering (CCECE)*, 2010. ISSN 0840-7789.

[7] HAMZAH, S.A.; BAHARUDIN, M.F.; SHAH, N.M..”Indoor channel prediction and measurement for wireless local area network (WLAN) system”. *In 2006 10th International Conference on Communication Technology*. Vols 1 and 2, Proceedings, 2006.

[8] KATULSKI, R.J.; LIPKA, A..”Methodology of radio signal power distribution modeling for WLAN networks.” In EUROCON 2007: The International Conference on Computer as a Tool, Vols 1-6, 2007.

[9] SADIKI, T.; PAIMBLANC, P..”Modelling new indoor propagation models for WLAN based on empirical results.” In UKSIM 2009: 11th International Conference on Computer Modelling and Simulation, 2009.

In case of shared authorship the co-authors contributed equally.

SUMMARY

This doctoral thesis addresses pre-assessment of EMC compliance with respect to radiated EMI from small horizontal submodules. It has been observed that the horizontal SB/MB structures are radiators of electric field due to the existing voltage potential V_{ant} between the submodule and the motherboard reference planes.

Traditional modelling approach is using field simulators to evaluated the maximum magnitude of the radiated electric field. However, the field simulators require a model of the SB/MB structure. This doctoral thesis introduces a novel simplified model which allows to simulate 3D pattern of the radiated electric field in reduced computation time through the replacement of the motherboard reference plane by an infinite plane. Based on the field simulations for various layouts of the interboard connector pins, following rule has been articulated: The more ground pins are available and the closer the ground pins are positioned mutually and towards the signal pin the tighter the current loops are and, hereby, the lower strengths of total radiated electric field occur.

In contrast to the latest modelling approaches, the author comes with a novel Radiation Model which determines the antenna transfer function from the Lumped-Element Equivalent circuit of the SB/MB structure. The transfer function can be determined from an analytically solution of the equivalent circuit (e.g. with PSPICE) and the radiated electric field strength is determined through the Antenna Model which is based on the Hertzian dipole. The same conclusions as achieved through the time consuming field simulations can be done by solving the Radiation Model in several minutes.

In order to further leverage from the fast prediction, the computation exercise with Radiation Model can be combined with a measurement method in a shielded box. This doctoral thesis introduces a novel concept of practical evaluation in a shielded box while as the receiver antenna a wideband planar spiral antenna is used which allows to perform a valuable pre-compliance assessment with the only means of usual measurement equipment. All novel modelling concepts in this thesis have been proved through the comparison with CISPR 22 EMI measurement in an anechoic chamber. Uncertainty of the estimation is sufficient for the EMC pre-compliance assessments.

RÉSUMÉ

Předmětem této dizertační práce je předběžné posouzení úrovně elektrického pole vyzářeného malým horizontálním modulem vzhledem k požadavkům na EMC. Pozorováním bylo zjištěno, že horizontální SB/MB struktura je zářičem elektrického pole, přičemž původcem je napěťový potenciál mezi nulovou úrovní na desce modulu a zemí na motherboardu.

Tradiční přístup k posouzení maximální úrovně vyzářeného elektrického pole pomocí modelování využívá simulátorů pole. Simulátory pole však vyžadují model struktury SB/MB. Tato dizertační práce představuje nový zjednodušený model, který umožňuje simulaci 3D obrazu elektrického pole v redukovaném výpočetním čase, kterého je dosaženo nahrazením motherboardu nekonečnou referenční rovinou. Na základě výsledků simulací pole provedených pro různá uspořádání pinů mezideskového konektoru bylo vysloveno následující pravidlo: Čím větší je počet zemnících pinů v konektoru a čím blíže jsou posazeny k sobě navzájem a vzhledem k signal pinu, tím užší jsou proudové smyčky a tím nižší je úroveň celkového vyzářeného elektrického pole.

Na rozdíl od nejnovějších přístupů k modelování elektromagnetického pole, autor přichází s novým vyzařovacím modelem, který určuje přenosovou funkci analytickým řešením náhradního obvodu struktury SB/MB, např. V programu PSPICE. Vyzářené elektrické pole lze určit pomocí anténního modelu vycházejícího z Hertzova dipólu. Ke stejným závěrům, kterých lze dosáhnout časově náročnými numerickými simulacemi pole, lze dospět pomocí řešení vyzařovacího modelu v několika minutách.

Za účelem pokročilejšího využití rychlé predikce, lze řešení vyzařovacího modelu zkombinovat s praktickým měřením ve stíněném boxu. Tato dizertační práce představuje unikátní koncept praktického měření ve stíněném boxu, přičemž anténu přijímače tvoří širokopásmová planární spirálová anténa, která umožňuje shodnocení EMC bilance běžnými měřícími prostředky. Platnost výsledků všech konceptů modelování elektrického pole představených v této dizertační práci byla ověřena srovnáním s referenčním měřením v bezodrazové anténní komoře podle požadavků CISPR 22. Nejistota odhadu je dostačující pro účely předběžného ohodnocení shody s EMC normami.